Propagation Over Parabolic Terrain: Asymptotics and Comparison to Data

Dmitry Chizhik, *Senior Member, IEEE*, Lawrence Drabeck, and W. Michael MacDonald, *Member, IEEE*

***Abstract*—Analysis of radio propagation over varying, clutter-covered terrain was carried out aiming at prediction of power received by a terminal immersed in clutter, with the transmitter placed above clutter. The need for such prediction arises, for example, in planning and assessing coverage and interference in radio communications. Following a general formulation of the problem, particular solutions were found when the terrain has constant curvature. Asymptotic evaluation yielded compact expressions both for parabolic valleys and ridges. In both cases, ray-optical term dominated for short ranges, while a single mode dominated at large ranges. Strong focusing was found to occur in valleys, while ridges produced strong blockage beyond the "horizon". The resulting procedure for predicting pathloss over varying terrain is therefore to apply the formulae using the terrain curvature extracted from terrain files. In comparison to measured power across a valley, mean errors of less than 1 dB were found, a marked improvement over standard terrain-unaware models that produce a mean error of 30 dB.**

***Index Terms*—Propagation, terrain factors.**

I. Introduction

PLANNING and performance assessment of radio communications often requires prediction of received power of both desired and interfering signals. A widely occurring arrangement is that of a transmitter (e.g. cellular base station) placed somewhat above terrestrial clutter and a terminal receiver immersed in clutter, such as buildings or trees. While prediction of exact received power requires unreasonably detailed knowledge of the environment as well as models of exceptionally high fidelity, it is often of interest to predict average received power that may be expected based on relatively crude information, such as terrain height variation and clutter height.

In the cellular industry a widespread practice is to employ empirical models of path loss such as [2]–[5]. These models were obtained through a reduction of measured path loss data and specify a linear relationship between pathloss in dB and the logarithm of transmitter-receiver separation. Resulting predictions are usually supplemented by adjusting the model parameters (i.e. slope and intercept) by fitting to locally measured data. Such practice leads to additional expense and delay of collecting data, but has the virtue of allowing for empirical adjustments due to unmodeled effects such as terrain and clutter variations.

Models based on first principles offer the promise of predictions without additional measurements. Examples of such models are the Walfisch-Bertoni model [6], derived for equal height buildings on flat terrain, and with buildings modeled as multiple absorbing half-screens. This was extended to buildings as screens on variable terrain [7]. Whitteker [8] has applied marching Huygens principle evaluation between elevated terrain points and included reflection from intervening terrain. This is a very general approach and is similar to parabolic equation methods [9], both involving iterative numerical computation as the field is "marched" in range. Blaunstein, *et al.* [10] represents propagation loss as a consequence of probabilistic visibility representation and interaction with multiple random scatterers. Blaunstein and Andersen [10] provide a extensive analysis of propagation over obstacles in rural areas, with each tree acting as a random phase-amplitude screen. Piazzi and Bertoni [12] extended [6] to variable terrain, exploring numerically the effect of clutter covered variable terrain with buildings represented as half-screens. Numerical solutions were found to be amenable to ray-optical interpretations. Barrios [21], Barrios *et al.* [22], Dockery and Kuttler, [23], Donohue and Kuttler [24] have applied the numerically efficient split-step/Fourier algorithm to generally varying terrain, allowing accounting both for terrain variation as well as atmospheric refraction at large ranges with no significant clutter.

In [1] local scattering around the mobile was treated in the case of flat terrain covered by constant height clutter. Present work is an extension of [1] aimed at allowing terrain height variation, particularly in the case of parabolic terrain, both in the case of a valley and a ridge. The goal is to derive relatively simple expressions for pathloss for this special case that wireless system planners would find useful and easy to use. The problem of solving for a field due to a source above a concave boundary, subject to the Dirichlet boundary condition has been treated by Felsen, *et al.* in [13] and [14]. It was found that the solution may be expressed asymptotically as a hybrid mix of rays and modes. In this work, it is of interest to find the received power for a terminal in terrestrial clutter. It was found in [1] that the key quantity of interest is the derivative of the Green's function at the clutter surface. In this work, the variable boundary problem is addressed through transforming the wave equation into a parabolic equation, which is then solved asymptotically to arrive at a hybrid ray-mode mixture. It is found that the solution has a simple interpretation of a ray optical contribution and only a single mode, other modes being negligible, both in the case of a

Manuscript received June 12, 2009; revised December 09, 2009; accepted December 10, 2009. Date of publication March 29, 2010; date of current version June 03, 2010.

The authors are with Bell Laboratories, Alcatel-Lucent, Holmdel, NJ 07733 USA.

Color versions of one or more of the figures in this paper are available online at http://ieeexplore.ieee.org.

Digital Object Identifier 10.1109/TAP.2010.2046855

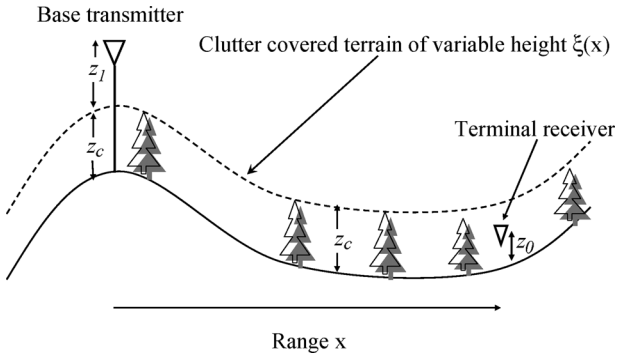

Fig. 1. Propagation over variable terrain.

concave and a convex boundary. The predictions are compared both to full modal sum solution as well as to measurements collected in variable terrain.

In Section II the problem of calculating fields in air over a generally rough dielectric surface is cast as a parabolic equation with a variable index of refraction. In Section III this equation is solved as a sum of modes for constant terrain curvature case (parabolic valley or ridge). In Section IV the sum of modes is found to be well approximated by a ray optical term and a single mode contribution, while Section V presents comparisons to measured power over a river valley.

II. Propagation in Air Over a Generally Varying Dielectric Surface

This work addresses prediction of average power received at a terminal beneath terrestrial clutter, such as trees and buildings, from a transmitter antenna placed at height z_1 above local clutter, where the terrain between the transmitter and the receiver is generally varying, illustrated in Fig. 1.

In [1] it was found that the received power P_R is related to the transmitted power P_T by

$$P_R = \lambda^2 \left\langle \left| \frac{\partial G}{\partial z'} \right|^2_{z'=0} \right\rangle L_{loc} P_T \tag{1}$$

where the mean square of the vertical derivative of the Green's function above clutter, $\langle |\partial G/\partial z'|^2_{z'=0} \rangle$, may be interpreted as the factor accounting for propagation over the clutter-covered varying terrain and the wavelength λ is related to the wavenumber k by $k = 2\pi/\lambda$. The local scattering factor

$$L_{loc} = \frac{A\pi}{4k^2(z_c - z_0)} \tag{2}$$

for the case of a terminal in the middle of a street of width A. The other quantities are local clutter height z_c and mobile height above local ground z_0, shown in Fig. 1. Similar expressions have also been found [1] for flat terrain covered by vegetation, as opposed to buildings.

For flat terrain with uniform height clutter, treated in [1], image theory has been used to determine $|\partial G/\partial z'|$. Letting the height of the base above clutter be z_1, and recognizing that for most cases of interest, $z_1 \ll x$, it was found that

$$\left\langle \left| \frac{\partial G}{\partial z'} \right|^2_{z'=0} \right\rangle \approx \frac{z_1^2}{\lambda^2 x^4} \tag{3}$$

Considering now the varying cluttered terrain boundary, the field $G(\mathbf{r})$ in air above the clutter due to a point source at $\mathbf{r_1}$ satisfies the Helmholtz equation

$$\nabla^2 G + k^2 G = \delta(\mathbf{r} - \mathbf{r_1}) \tag{4}$$

The top of the surface may be viewed as an inhomogeneous dielectric whose height $\xi(x)$ varies as a function of range x. It may be noted, however, that for a large range of material properties and for both polarizations, plane wave incidence at small grazing angles results in nearly perfect reflection, with a reflection coefficient of nearly -1. The interaction with a surface is then approximated here as the Dirichlet boundary condition

$$G\left(x, y, \xi(x)\right) = 0 \tag{5}$$

The problem may be transformed into a simpler problem by substituting

$$G(\mathbf{r}) = E(\mathbf{r}) e^{ikx} \tag{6}$$

into (4) to get

$$2ik\frac{\partial E}{\partial x} + \frac{\partial^2 E}{\partial x^2} + \frac{\partial^2 E}{\partial y^2} + \frac{\partial^2 E}{\partial z^2} = \delta(\mathbf{r} - \mathbf{r_1}) \tag{7}$$

Assuming nearly grazing propagation, $(\partial^2 E/\partial x^2) \ll 2ik(\partial E/\partial x)$, (7) becomes the "parabolic equation"

$$2ik\frac{\partial E}{\partial x} + \frac{\partial^2 E}{\partial y^2} + \frac{\partial^2 E}{\partial z^2} = \delta(\mathbf{r} - \mathbf{r_1}) \tag{8}$$

or a Schrödinger's equation with two spatial dimensions y and z, and range x playing the role of time. A transformation proposed by Beillis and Tappert [8] allows further simplification. Letting

$$z' = z - \xi(x) \tag{9}$$

and substituting

$$E(\mathbf{r}) = G_1(\mathbf{r}) \exp\left(ik\dot{\xi}(x)z' + i\int_{x_1}^{x} dx'' \frac{1}{2} k\dot{\xi}^2(x'') \right) \tag{10}$$

into (8), results in

$$2ik\frac{\partial G_1}{\partial x} + \frac{\partial^2 G_1}{\partial y^2} + \frac{\partial^2 G_1}{\partial z^2} - 2k^2\ddot{\xi}(x) z G_1 = \delta(x, y, z - z_1) \tag{11}$$

where the prime notation on z' is omitted for notational clarity. The boundary condition (5) is transformed by (9) to a flat surface boundary condition:

$$G_1(x, y, 0) = 0 \tag{12}$$

The balance of the work addresses particular solutions of (11) with (12) as the boundary condition.

III. Constant Terrain Curvature

A. Sum of Modes Solution

Of particular interest is the case of constant curvature terrain, $\ddot{\xi}(x) = \ddot{\xi}$, corresponding to a parabolic valley ($\ddot{\xi} > 0$) or a parabolic ridge ($\ddot{\xi} < 0$). Equation (11) subject to (12) may be solved [16], [17] by introducing a horizontal Green's function $G_{\mathrm{H}}(x, y|x_1, y_1)$, describing the field at (x, y) due to a point source at (x_1, y_1), and a vertical Green's function $G_{\mathrm{V}}(z|z_1)$ due to a point source at z_1. The two Green's functions satisfy correspondingly

$$2ik\frac{\partial G_{\mathrm{H}}}{\partial x} + \frac{\partial^2 G_{\mathrm{H}}}{\partial y^2} - k_{\mathrm{V}}^2 G_{\mathrm{H}} = \delta(x - x_1, y - y_1) \tag{13}$$

and

$$\frac{\partial^2 G_{\mathrm{V}}}{\partial z^2} + \left(k_{\mathrm{V}}^2 - 2k^2\ddot{\xi}z\right) G_{\mathrm{V}} = \delta(z - z_1) \tag{14}$$

where the separation constant k_{v}^2 may be interpreted as a square of the vertical component of the wavevector. The solution to (11) may be expressed as

$$G_1 = \frac{1}{2\pi i}\oint dk_{\mathrm{v}}^2 G_{\mathrm{H}}\left(k_{\mathrm{v}}^2, x, y\right) G_{\mathrm{V}}\left(k_{\mathrm{v}}^2, z|z_1\right). \tag{15}$$

The contour integral in (15) encompasses the poles of the vertical Green's function $G_{\mathrm{V}}(k_{\mathrm{v}}^2, z|z_1)$. The coordinates of the source (base antenna) in the horizontal plane have been set to $(x_1, y_1) = (0, 0)$ in (15) for convenience.

Equation (13) may be solved using Fourier transforms to yield

$$G_{\mathrm{H}}\left(k_{\mathrm{V}}^2, x, y\right) = \frac{1}{4\pi ik}\sqrt{\frac{2\pi k}{ix}} e^{-i\frac{k_{\mathrm{V}}^2 x}{2k}} e^{i\frac{ky^2}{2x}} \tag{16}$$

The solution to (15) may be expressed as a sum over residues at the poles of the integrand in (15):

$$G_1(x, y, z) = \sum_l G_{\mathrm{H}}\left(k_{\mathrm{V}_l}^2, x, y\right) \frac{g\left(k_{\mathrm{V}_l}^2, z\right) g\left(k_{\mathrm{V}_l}^2, z_1\right)}{\frac{\partial \mathrm{w}}{\partial\left(k_{\mathrm{V}_l}^2\right)}} \tag{17}$$

recognized as a sum over modes where $g(k_{\mathrm{V}_l}^2, z)$ is the vertical mode function of the l^{th} mode, satisfying the source-free version of (14) and the boundary condition (12), with the corresponding Wronskian determinant [18]:

$$\mathrm{w} = g\left(k_{\mathrm{V}_l}^2, z\right)\frac{\partial g\left(k_{\mathrm{V}_l}^2, z\right)}{\partial z} \tag{18}$$

and

$$\frac{\partial \mathrm{w}\left(k_{\mathrm{V}_l}^2\right)}{\partial k_{\mathrm{V}_l}^2}\bigg|_{z=0} = \frac{\partial g\left(k_{\mathrm{V}_l}^2, z\right)}{\partial k_{\mathrm{V}_l}^2}\frac{\partial g\left(k_{\mathrm{V}_l}^2, z\right)}{\partial z}\bigg|_{z=0}. \tag{19}$$

The received power (1) depends on the absolute value of the z-derivative of the Green's function $G(x, y, z)$ at the surface. As may be observed from (6) and (10)

$$\begin{aligned}\left|\frac{\partial G}{\partial z}\right|_{z=0}^2 &= \left|\frac{\partial G_1(x, y, z)}{\partial z} + ik\dot{\xi}(x)G_1(x, y, z)\right|_{z=0}^2 \\ &= \left|\frac{\partial G_1(x, y, z)}{\partial z}\right|_{z=0}^2\end{aligned} \tag{20}$$

where the last equality follows from the boundary condition (12). The z-derivative of (17), where only $g(k_{\mathrm{V}_l}^2, z)$ depends on z, is, then, using (19),

$$\begin{aligned}\frac{\partial G_1(x, y, z)}{\partial z}\bigg|_{z=0} &= \sum_l G_{\mathrm{H}}\left(k_{\mathrm{V}_l}^2, x, y\right) \\ &\quad\times \frac{\frac{\partial g\left(k_{\mathrm{V}_l}^2, z\right)}{\partial z}\Big|_{z=0} g\left(k_{\mathrm{V}_l}^2, z_1\right)}{\frac{\partial g\left(k_{\mathrm{V}_l}^2, z\right)}{\partial z}\Big|_{z=0}\frac{\partial g\left(k_{\mathrm{V}_l}^2, 0\right)}{\partial k_{\mathrm{V}_l}^2}} \\ &= \sum_l G_{\mathrm{H}}\left(k_{\mathrm{V}_l}^2, x, y\right) f\left(k_{\mathrm{V}_l}^2, z_1\right)\end{aligned} \tag{21}$$

where

$$f\left(k_{\mathrm{V}_l}^2, z_1\right) = \frac{g\left(k_{\mathrm{V}_l}^2, z_1\right)}{\frac{\partial g\left(k_{\mathrm{V}_l}^2, 0\right)}{\partial k_{\mathrm{V}_l}^2}} \tag{22}$$

is defined for later convenience. The form of the vertical mode function $g(k_{\mathrm{V}_l}^2, z_1)$ depends on the sign of the terrain curvature, as described in the following sections.

B. Valley ($\ddot{\xi} > 0$)

In the case of a valley, vertical mode solutions $g(k_{\mathrm{V}_l}^2, z)$ satisfying the source-free version of (14) are Airy functions [18]

$$g\left(k_{\mathrm{V}_l}^2, z\right) = Ai\left(z/H - k_{\mathrm{V}_l}^2 H^2\right) \tag{23}$$

where the effective waveguide width

$$H = 1/(2\ddot{\xi}k^2)^{\frac{1}{3}} \tag{24}$$

depends on the curvature $\ddot{\xi}$ and the characteristic vertical spatial frequency k_{V_l} is determined from boundary condition $g(k_{\mathrm{V}_l}^2, z) = 0$ to be approximately [18] defined by

$$k_{\mathrm{V}_l}^3 H^3 \approx \frac{3\pi}{2}\left(l - \frac{1}{4}\right). \tag{25}$$

C. Ridge ($\ddot{\xi} < 0$)

In the case of a ridge, the vertical mode solutions $g(k_{\mathrm{V}_l}^2, z)$ satisfying the source-free version of (14) are Airy functions with complex arguments [18]

$$g\left(k_{\mathrm{V}_l}^2, z\right) = 2Ai\left(\left(z/H + k_{\mathrm{V}_l}^2 H^2\right)e^{-i\pi/3}\right)e^{i\pi/6} \tag{26}$$

where $H = 1/(2|\ddot{\xi}|k^2)^{1/3}$ depends on the curvature $\ddot{\xi}$ and the characteristic vertical spatial frequency k_{V_l} is determined [18] from boundary condition $g(k_{\mathrm{V}_l}^2, z) = 0$ to approximately satisfy

$$k_{\mathrm{V}_l}^3 H^3 \approx -\frac{3\pi}{2}\left(l - \frac{1}{4}\right). \tag{27}$$

IV. Asymptotic Evaluation

A. Valley ($\ddot{\xi} > 0$)

While summation over modes in (21) may be carried out directly, the number of terms that are needed is often large, particularly for short ranges and/or small terrain curvatures. It is therefore of interest to derive an asymptotic expression that would provide approximate yet accurate results. This may be obtained by recognizing that the Airy function $Ai(t)$ has the following asymptotic representation [18], [19] for large values of $|t|$

$$Ai(t) = \begin{cases} \frac{e^{-\frac{2}{3}t^{3/2}}}{2\sqrt{\pi}t^{1/4}}, & |\arg(t)| < \frac{2\pi}{3} \\ \frac{\sin\left(\frac{2}{3}(-t)^{3/2} + \frac{\pi}{4}\right)}{\sqrt{\pi}(-t)^{1/4}}, & |\arg(-t)| < \frac{2\pi}{3} \end{cases}. \tag{28}$$

The summation over the modes (21) may now be split into two sums, one for each of the regions in (28):

$$\left.\frac{\partial G_1(x,y,z)}{\partial z}\right|_{z=0} = I_1 + I_2 \tag{29}$$

where terms for $k_{\mathrm{V}_l}^2 < k_{WG}^2$ are summed in

$$I_1 = \sum_{k_{\mathrm{V}_l}^2 = k_{\mathrm{V}_1}^2}^{k_{\mathrm{V}_l}^2 = k_{WG}^2} G_{\mathrm{H}}\left(k_{\mathrm{V}_l}^2, x, y\right) f\left(k_{\mathrm{V}_l}^2, z_1\right) \tag{30}$$

and terms for $k_{\mathrm{V}_l}^2 > k_{WG}^2$ are summed in

$$I_2 = \sum_{k_{\mathrm{V}_l}^2 \simeq k_{WG}^2}^{k_{\mathrm{V}_l}^2 = \infty} G_{\mathrm{H}}\left(k_{\mathrm{V}_l}^2, x, y\right) f\left(k_{\mathrm{V}_l}^2, z_1\right) \tag{31}$$

where $k_{WG}^2 \approx (z_1/H^3)$, with the subscript indicating the dominant "whispering gallery" mode and mode functions (23) are used.

Now using the asymptotic form (28), one finds that for $k_{\mathrm{V}_l}^2 H^2 > z_1/H$

$$\begin{aligned} Ai\left(-k_{\mathrm{V}_l}^2 H^2 + z/H\right) &\approx \frac{\sin\left(\frac{2}{3}\left(k_{\mathrm{V}_l}^2 H^2 - z/H\right)^{3/2} + \frac{\pi}{4}\right)}{\sqrt{\pi}\left(k_{\mathrm{V}_l}^2 H^2 - z/H\right)^{1/4}} \\ &\approx \frac{\sin\left(\frac{2}{3}k_{\mathrm{V}_l}^3 H^3 - k_{\mathrm{V}_l} z + \frac{\pi}{4}\right)}{\sqrt{\pi}\left(k_{\mathrm{V}_l}^2 H^2\right)^{1/4}}. \end{aligned} \tag{32}$$

Where the expression in the numerator was expanded to first order in the Taylor series for $k_{\mathrm{V}_l}^2 H^3 \gg z$. In the last approximation in (32) the z-dependence of the denominator is neglected in comparison to the rapid fluctuation of the numerator with respect to z. Using (25) for the characteristic spatial frequencies k_{V_l}, the asymptotic behavior of vertical mode function (32) may be seen to be

$$\begin{aligned} &Ai\left(-k_{\mathrm{V}_l}^2 H^2 + z/H\right) \\ &\quad\approx \frac{e^{-\frac{2}{3}\left(z/H - k_{\mathrm{V}_l}^2 H^2\right)^{3/2}}}{2\sqrt{\pi}\left(z/H - k_{\mathrm{V}_l}^2 H^2\right)^{1/4}}, \quad k_{\mathrm{V}_l}^2 H^2 < z/H \\ &\quad\approx (-1)^{l+1}\frac{\sin\left(k_{V_l} z\right)}{\sqrt{\pi}\sqrt[4]{k_{\mathrm{V}_l}^2 H^2}}, \quad k_{\mathrm{V}_l}^2 H^2 > z/H. \end{aligned} \tag{33}$$

The denominator of (22) used in (31) depends on the behavior of the Airy function near $z = 0$ and may thus be evaluated using the second approximation in (32) to be

$$\left.\frac{\partial Ai\left(-k_{\mathrm{V}_l}^2 H^2 + z/H\right)}{\partial\left(k_{\mathrm{V}_l}^2\right)}\right|_{z=0} \approx (-1)^l \frac{H^2\sqrt[4]{k_{\mathrm{V}_l}^2 H^2}}{\sqrt{\pi}}. \tag{34}$$

Substituting 1st expression in (33), (34) into (30) and (31), leads to

$$\begin{aligned} I_1 &= \sum_{k_{\mathrm{V}_l}^2 = k_{\mathrm{V}_1}^2}^{k_{\mathrm{V}_l}^2 = k_{WG}^2} \frac{1}{4\pi i k}\sqrt{\frac{2\pi k}{ix}} e^{-i\frac{k_{\mathrm{V}_1}^2 x}{2k}} e^{i\frac{ky^2}{2x}} f\left(k_{\mathrm{V}_l}^2, z_1\right) \\ &\approx \sum_{k_{\mathrm{V}_l}^2 = k_{\mathrm{V}_1}^2}^{k_{\mathrm{V}_l}^2 = k_{WG}^2} \frac{1}{4\pi i k}\sqrt{\frac{2\pi k}{ix}} e^{-i\frac{k_{\mathrm{V}_1}^2 x}{2k}} e^{i\frac{ky^2}{2x}} (-1)^l \\ &\quad\times \frac{e^{-\frac{2}{3}\left(z_1/H - k_{\mathrm{V}_l}^2 H^2\right)^{3/2}}}{2H^2\left(z_1/H - k_{\mathrm{V}_l}^2 H^2\right)^{1/4}\left(k_{\mathrm{V}_l}^2 H^2\right)^{1/4}} \end{aligned} \tag{35}$$

and similarly using 2nd expression in (33)

$$I_2 = \sum_{k_{\mathrm{V}_l}^2 \simeq k_{WG}^2}^{k_{\mathrm{V}_l}^2 = \infty} \frac{1}{4\pi i k}\sqrt{\frac{2\pi k}{ix}} e^{-i\frac{k_{\mathrm{V}_1}^2 x}{2k}} e^{i\frac{ky^2}{2x}} \frac{\sin\left(k_{V_l} z\right)}{H^2\sqrt[2]{k_{\mathrm{V}_l}^2 H^2}}. \tag{36}$$

At short ranges, the terms in the sum (35) vary slowly with mode index l, with the exception of the factor $(-1)^l$, which leads to near cancellation of the successive terms. The resulting "telescoping" series thus has only the first and the last terms in the sum that offer significant contribution. The last term corresponds to the characteristic spatial frequency given by $k_{\mathrm{V}_l}^2 = k_{WG}^2$. The first term, corresponding to the lowest order mode, may be seen in (35) to be exponentially smaller than the last term, and is neglected. At larger ranges, the phase differences between modes due to the term $e^{-i(k_{\mathrm{V}_1}^2 x/2k)}$ become important, making it necessary to include more modes. From (35) it may be seen that the dominant contribution comes from modes with characteristic vertical spatial frequencies in the neighborhood of $k_{\mathrm{V}_l}^2 = k_{WG}^2 \sim z_1/H^3$. The dominant mode contribution is

$$I_1 \approx \frac{1}{4\pi i k}\sqrt{\frac{2\pi k}{ix}} e^{-i\frac{k_{WG}^2 x}{2k}} e^{i\frac{ky^2}{2x}} f\left(k_{WG}^2, z_1\right) \tag{37}$$

where

$$k_{\mathrm{WG}}^3 H^3 \approx \frac{3\pi}{2}\left(l_{WG}-\frac{1}{4}\right) \tag{38}$$

and

$$l_{WG}=\max_l \left|Ai\left(-k_{V_l}^2H^2+z_1/H\right)\right|. \tag{39}$$

The sum in (36) is now examined. The difference in the square of the spatial frequencies of neighboring modes may be deduced from (25) as

$$\Delta k_{V_l}^2 = k_{V_{l+1}}^2 - k_{V_l}^2 \approx \frac{\pi}{H^3 k_{V_l}} \tag{40}$$

leading to $\Delta k_{V_l}^2 (H^3 k_{V_l}/\pi)\approx 1$. This may be used to approximate the sum into an integral over a continuum of characteristic spatial frequencies:

$$I_2 \approx \int_{k_{WG}^2}^{\infty} d(k_{V_l}^2)\frac{H^3 k_{V_l}}{\pi}\frac{1}{4\pi i k}\sqrt{\frac{2\pi k}{ix}}e^{-i\frac{k_{V_l}^2 x}{2k}}e^{i\frac{ky^2}{2x}}\frac{\sin\left(k_{V_l}z\right)}{H^2\sqrt[2]{k_{V_l}^2H^2}}. \tag{41}$$

The integral in (41) may be approximated by representing the sin as a sum of two complex exponentials and using stationary phase techniques to evaluate the integral asymptotically, resulting in

$$\left.\frac{\partial G_1(x,y,z)}{\partial z}\right|_{z=0} \approx \frac{1}{4\pi i k}\sqrt{\frac{2\pi k}{ix}}e^{-i\frac{k_{WG}^2 x}{2k}}e^{i\frac{ky^2}{2x}}f\left(k_{WG}^2,z_1\right) + e^{i\frac{ky^2}{2x}}\frac{z_1}{i\lambda x^2}U\left(k\frac{z_1}{x}-k_{WG}\right) \tag{42}$$

where the Heavyside step function U is introduced to indicate that in the stationary phase approximation, the integral I_2 contributes only when the stationary phase point $k_V = kz_1/x$ is within the limits of the integral (41). The signal arriving at the receiver may be thought of as consisting of two parts: the "whispering gallery mode", represented by the first term I_1, significant at large ranges, and the ordinary optical term I_2, corresponding to the superposition of the direct and reflected from the top of the clutter paths. The ordinary optical term is significant at shorter ranges, and, within the approximations used here, corresponds to the case of the flat terrain used in (3). More precise evaluation of (41) may be obtained from higher order asymptotic evaluations of the integral, which would remove the abrupt transition indicated by the step function. It has been found that a simple approximation may be obtained by recognizing that each of the two terms in (42) dominates in a different range of source-receiver separation x, with a switch occurring around $x_{crit}\approx kz_1/k_{WG}$ It is decided here in an ad hoc manner to remove the step function U, resulting in

$$\left.\frac{\partial G_1(x,y,z)}{\partial z}\right|_{z=0} \approx \frac{e^{i\frac{ky^2}{2x}}}{4\pi i k}\sqrt{\frac{2\pi k}{ix}}e^{-i\frac{k_{WG}^2 x}{2k}}f\left(k_{WG}^2,z_1\right) + e^{i\frac{ky^2}{2x}}\frac{z_1}{i\lambda x^2}. \tag{43}$$

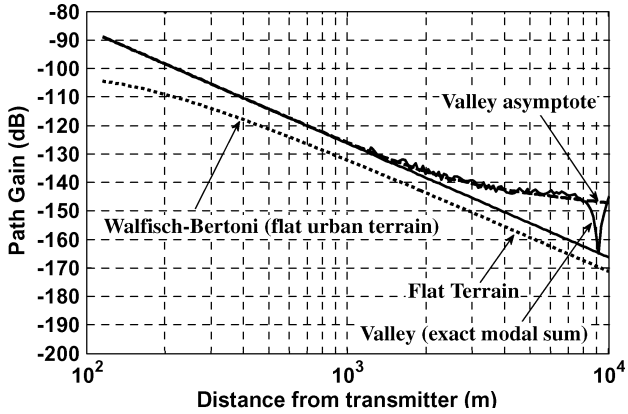

Fig. 2. Path gain as a function of range for various models over flat terrain and a parabolic valley. 2 GHz, Transmitter height 20 m, Clutter height 9 m, receiver height 2 m, terrain curvature $2\times 10^{-6}\ \mathrm{m}^{-1}$

The last step is justified through a numerical comparison of (43) with the complete modal sum solution (17).

Finally, the quantity of interest for evaluating the average received signal power (1) is

$$\left\langle\left|\frac{\partial G_1(x,y,z)}{\partial z}\right|_{z=0}^2\right\rangle \approx |I_1|^2+|I_2|^2 \approx \frac{1}{8\pi kx}f\left(k_{WG}^2,z_1\right)+\frac{z_1^2}{\lambda^2x^4} \tag{44}$$

where the cross term $2\langle \mathrm{Re}[I_1 I_2^*]\rangle$ has been set to zero under the assumption that the relative phase between the whispering gallery mode field I_1 and the ordinary optical contribution I_2 will depend significantly on the precise shape of the top of the clutter boundary and is assumed to be uniformly distributed.

Using (44), the received power in (1) the case of the valley may therefore be expressed as

$$P_R = \lambda^2\frac{1}{8\pi kx}\left|f\left(k_{WG}^2,z_1\right)\right|^2 L_{loc}P_T + \frac{z_1^2}{x^4}L_{loc}P_T \tag{45}$$

where $f(k_{WG}^2,z_1)$ is defined in (22) with the mode function $g(k_{WG}^2,z)$ as in (23) and using (38). Also, L_{loc} defined in (2) for areas with buildings and by (29) in [1] for dense vegetation.

In Fig. 2, the asymptotic result (45) is compared to the exact sum over modes (1), (21), (23), (25). Also plotted for comparison are flat terrain predictions [1] as well as the widely used Walfisch-Bertoni model [6], derived for propagation over flat urban terrain with equal height buildings, modeled as absorbing half-screens. Okumura-Hata model [2]–[4], gives similar results to the flat-terrain and Walfisch-Bertoni models, as discussed in [1]. It may be observed that while all models give similar predictions at shorter ranges, guiding by the valley results in signals that are over 20 dB stronger at 10 km. The exact sum of modes solution to propagation over a valley produces "beating" between modes, resulting in some oscillation in path gain as a function of range. Nevertheless, the asymptotic formula (45) captures the exact sum of modes behavior quite well.

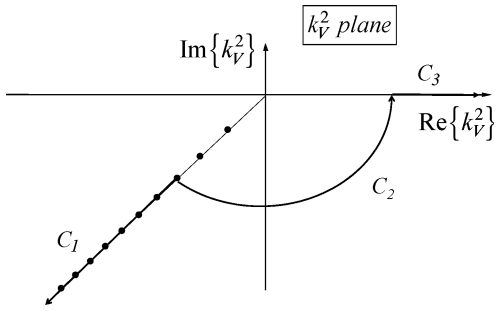

Fig. 3. Characteristic spatial frequencies and integration contours.

B. Ridge ($\ddot{\xi} < 0$)

In the case of a ridge, the modal expansion (21) may be expressed using (16) and (26) as

$$\left.\frac{\partial G_1(x,y,z)}{\partial z}\right|_{z=0} = \sum_l \frac{1}{4\pi ik}\sqrt{\frac{2\pi k}{ix}} e^{-i\frac{k_{V_l}^2 x}{2k}} e^{i\frac{ky^2}{2x}} f\left(k_{V_l}^2, z_1\right). \tag{46}$$

The characteristic vertical spatial frequencies $k_{V_l}^2$ (27) are located [18] on a ray $[0,\infty]e^{-i2\pi/3}$ depicted in the third quadrant of Fig. 3.

The asymptotic evaluation of (46) may be carried out by separating the sum over modes into two groups, $k_{V_l}^2 \in [k_{V_1}^2, z_1/H^3]e^{-i2\pi/3}$ and $k_{V_l}^2 \in (z_1/H^3,\infty]e^{-i2\pi/3}$, motivated by the change in the Airy function behavior, as described by (28)

$$\left.\frac{\partial G_1(x,y,z)}{\partial z}\right|_{z=0} = \sum_{k_{V_l}^2 \in \left[k_{V_1}^2, z_1/H^3\right]e^{i2\pi/3}} (\ldots) + \sum_{k_{V_l}^2 \in (z_1/H^3,\infty]e^{i2\pi/3}} (\ldots) \tag{47}$$

where the summand expression from (46) is not written explicitly for compactness. The second sum in (47) is now approximated by an integral over the continuous range $(z_1/H^3,\infty]e^{-i2\pi/3}$, denoted as the contour C_1 in Fig. 3

$$\left.\frac{\partial G_1(x,y,z)}{\partial z}\right|_{z=0} = \sum_{k_{V_l}^2 \in \left[k_{V_1}, \frac{z_1}{H^3}\right]e^{-i2\pi/3}} (\ldots) + \int_{C_1} d\left(k_V^2\right) \frac{H^3 k_{V_l}}{\pi}(\ldots) \tag{48}$$

where the modal density $H^3 k_{V_l}/\pi$ is introduced using (40) and following the argument leading to (41). The integrand in the contour integral in (48) is analytic in the region $\arg\{k_V^2\} \in [2\pi/3, 2\pi]$, allowing for the changing of the contour from C_1 to $C_2 + C_3$. Using the asymptotic form of the Airy function (28), this results in

$$\left.\frac{\partial G_1(x,y,z)}{\partial z}\right|_{z=0} = \sum_{k_{V_l}^2 \in \left[k_{V_1}, \frac{z_1}{H^3}\right]e^{-i2\pi/3}} (\ldots) + \int_{C_2+C_3} d\left(k_V^2\right) \frac{H^3 k_{V_l}}{\pi}(\ldots). \tag{49}$$

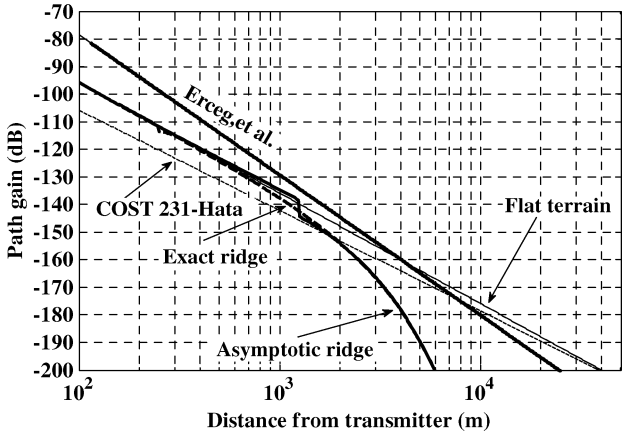

Fig. 4. Path gains predicted by accepted models, flat terrain model, and ridge models. Various heights are: Transmitter 20 m, Clutter 9 m, receiver 2 m, terrain curvature -3.2×10^{-6} m^{-1}

It may be shown that the integral over the contour C_2 is exponentially smaller than other terms and is therefore neglected here. The integral over C_1 is the same as (41), and may therefore be evaluated approximately through a stationary phase technique in the same way. Each of the discrete modes in the sum in (49) decays exponentially with range, corresponding to the shedding of energy by creeping waves [20]. The lowest order mode suffers the least decay and all higher order modes are here neglected. These considerations allow the vertical derivative of the Greens function (49) to be approximated as a sum of the ordinary ray-optical component and the lowest order creeping wave

$$\left.\frac{\partial G_1(x,y,z)}{\partial z}\right|_{z=0} \approx e^{i\frac{ky^2}{2x}}\frac{z_1}{i\lambda x^2} U\left(k\frac{z_1}{x} - \sqrt{z_1/H^3}\right) + \frac{1}{4\pi ik}\sqrt{\frac{2\pi k}{ix}} e^{-i\frac{k_{V_1}^2 x}{2k}} e^{i\frac{ky^2}{2x}} f\left(k_{V_l}^2, z_1\right). \tag{50}$$

The step function in (50) indicates that, in the stationary phase approximation, the second integral in (48) contributes only when the stationary phase point is within the limits of the integral. Finally, substituting (50) in (1) results in the power received by an antenna buried in the clutter approximated as

$$P_R = L_{loc} P_T \lambda^2 \frac{1}{8\pi kx}\left|f\left(k_{V_l}^2, z_1\right)\right|^2 e^{\frac{-\mathrm{Im}\left\{k_{V_1}^2\right\}x}{k}} + \frac{z_1^2}{x^4} L_{loc} U\left(k\frac{z_1}{x} - \sqrt{z_1/(2H^3)}\right) P_T \tag{51}$$

where $f(k_{V_l}^2, z_1)$ is defined in (22) with the mode function $g(k_{V_l}^2, z)$ as in (26) and k_{V_1} for $l = 1$ mode given by (27). Also, L_{loc} defined in (2) for areas with houses and by (29) in [1] for dense vegetation. The step function in (51) has the effect of removing the contribution of the ordinary optical term at large ranges, $x > k\sqrt{2z_1H^3} = \sqrt{z_1/\ddot{\xi}}$, interpreted as blockage by the ridge. Path gain predicted by several models is shown in Fig. 4. The exact solution, computed from a sum of residues (46) is indicated as a thick dashed line in Fig. 4 follows the flat terrain model for short ranges, but shows increasingly larger

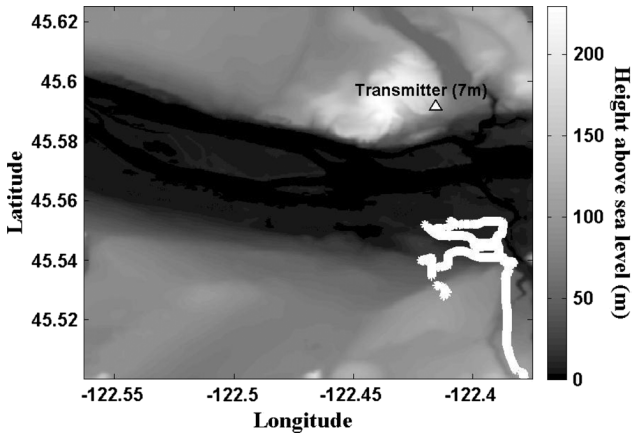

Fig. 5. Terrain height across the Columbia river, Portland OR. Transmitter is marked as a white triangle, receiver locations as white stars.

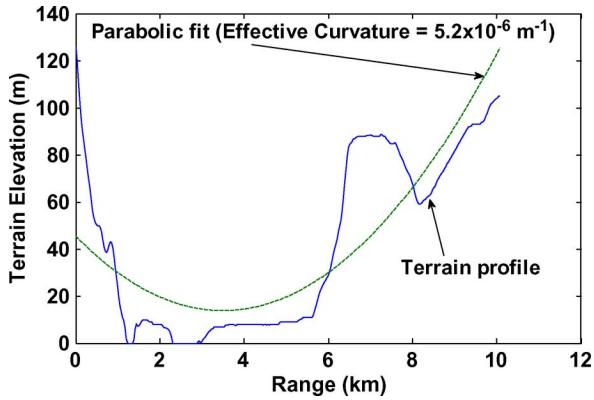

Fig. 6. Actual terrain profile across the river valley and its parabolic fit (curvature of $5.2 \times 10^{-6}\ \mathrm{m}^{-1}$)

loss at larger ranges. The asymptotic ridge solution (51) follows closely the exact solution at both large and small ranges, with the exception of the transition around 1 km, where the ray-optical contribution is blocked by the terrain. Higher order asymptotic evaluation of the integral over C_1 in (49) may allow further improvement in agreement, which is not pursued here. Similar conclusions have been reached in Piazzi and Bertoni [12] where a marching diffraction solution over sequences of half-screens over variable terrain were found to be well approximated by corresponding ray-optical expressions similar in form to that obtained for diffraction over smooth cylinders.

V. Comparison With Measurements

Received power was measured as part of a data collection campaign carried out in Portland, Oregon. Grey scale illustration of terrain height, together with locations of transmitter and receivers is in Fig. 5. The transmitter was a 7 m high, 20 W, 120° sector antenna radiating at 1.9 GHz, placed on the north bank of the Columbia river, Fig. 5, aimed south across the river. The receiver was an omnidirectional antenna placed on a roof of a vehicle and driven on the roads on the south bank. The terrain along a typical vertical profile from the transmitter to the measurement area is shown in Fig. 6. A parabolic fit to the terrain profile provides the value of terrain curvature $\ddot{\xi}$ needed

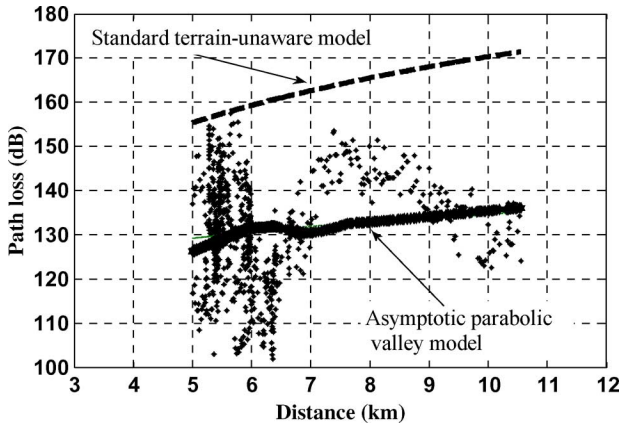

Fig. 7. Measured (stars) and predicted pathloss as a function of range (linear scale) at 1.9 GHz. Predictions are made using a standard (terrain-unaware) model [5] and asymptotic valley prediction.

to define H in (24). Terrain variations that deviate from the parabola are not treated here. Pathloss predicted using (45) as well as a standard (terrain-unaware) model [5] is compared against measurements as a function of the separation range x in Fig. 7, with range plotted on a linear scale for clarity. Measured power discussed here is actually a local average of the instantaneous values of received signal power, a process that largely removes small scale variations and leaves only the slower variations of average power of interest here. Measured received power is observed to deviate significantly from predictions, with the error having a standard deviation of 14 dB, attributed to the unmodeled terrain variations, beyond the simple parabolic shape. Nevertheless, the model (45) results in a small mean error (<1 dB). Standard model results in a mean error of 30 dB, underscoring the importance of modeling the whispering gallery modes guided by the valley. Similarly large errors would result from the use of any standard terrain-unaware model.

Clearly, further modeling is required to account for general terrain variations, perhaps through numerical solutions of the parabolic wave (11). Solutions of the parabolic equation using the very efficient split step algorithm have been applied to predicting field strengths over variable terrain and variable refractivity in [21]–[24]. Model accuracy was assessed through comparison to measurements carried out mostly in areas of negligible vegetation. Clutter such as vegetation would have two primary effects on propagation: raising of the effective terrain height to that of clutter top and changing the propagation mechanism at the mobile from direct illumination to scattering [1]. At 2 GHz these effects exceed 30 dB. Extending the numerical solutions of the parabolic wave equation to include the effects of scattering into clutter would be a promising combination of proper treatment of general terrain and proper treatment of near-mobile scattering. More generally, numerical solutions offer treatment of arbitrary terrain variation while analytical methods, such as presented here, offer insight in certain canonical cases. The work presented here is aimed at the extension of flat terrain formulations [1], [2], [4], [6], some widely used, to include terrain curvature, where it is important.

VI. Conclusion

Analysis of radio propagation over varying, clutter-covered terrain was carried out, for the case when one end of the radio link, e.g. a receiver, is immersed in clutter. Asymptotic evaluation yielded compact expressions for received power for constant curvature terrain, i.e. parabolic valleys and ridges. For both cases, ray-optical term dominated for short ranges, while a single mode dominated at large ranges. Strong focusing was found to occur in valleys, while ridges produced strong blockage beyond the "horizon". Presented closed-form expressions for pathloss require terrain curvature as a parameter. Terrain curvature may be obtained from a parabolic fit to the terrain profile available from a terrain elevation database. In the limit of zero curvature, the pathloss formulas match flat terrain predictions. In comparison to measured power across a valley, mean errors of less than 1 dB were found, a marked improvement over standard terrain-unaware models that produce a mean error of 30 dB. Still, large standard deviation of error points to a need to account for general terrain variations, beyond the parabolic case.

Acknowledgment

The authors wish to thank A. Diaz for his insightful comments that have improved and enriched the theoretical treatment.

References

[1] D. Chizhik and J. Ling, "Propagation over clutter: Physical stochastic model," *IEEE Trans. Antennas Propag.*, vol. 56, no. 4, pp. 1071–1077, April 2008.

[2] M. Hata, "Empirical formula for propagation loss in land mobile radio services," *IEEE Trans. Veh. Tech.*, vol. 29, no. 3, pp. 317–325, Aug. 1980.

[3] Y. Okumura, E. Ohmori, T. Kawano, and K. Fukuda, "Field strength and its variability in VHF and UHF land-mobile radio service," *Rev. Elec. Com. Lab.*, vol. 16, pp. 825–873, 1968.

[4] COST Action 231, "Digital Mobile Radio Towards Future Generation Systems, Final Report," European Communities, EUR 18957, 1999, technical report.

[5] V. Erceg, L. J. Greenstein, S. Y. Tjandra, S. R. Parkoff, A. Gupta, B. Kulic, A. A. Julius, and R. Bianchi, "An empirically based path loss model for wireless channels in suburban environments," *IEEE J. Sel. Areas Commun.*, vol. 17, no. 7, pp. 1205–1211, Jul. 1999.

[6] J. Walfisch and H. L. Bertoni, "A theoretical model of UHF propagation in urban environments," *IEEE Trans. Antennas Propag.*, vol. 36, no. 12, pp. 1788–1796, Dec. 1988.

[7] L. Piazzi and H. L. Bertoni, "Effect of terrain on path loss in urban environments for wireless applications," *IEEE Trans. Antennas Propag.*, vol. 46, pp. 1138–1147, Aug. 1998.

[8] J. H. Whitteker, "Physical optics and field-strength predictions for wireless systems," *IEEE J. Sel. Areas Commun.*, vol. 20, no. 3, pp. 515–522, Apr. 2002.

[9] M. Levy, *Parabolic Equation Methods for Electromagnetic Wave Propagation*. Stevenage, U.K.: IEE, 2000, p. 353.

[10] N. Blaunstein, D. Katz, D. Censor, A. Freedman, I. Matityahu, and I. Gur-Arie, "Prediction of loss characteristics in built-up areas with various buildings' overlay profiles," *IEEE Antennas Propag. Mag.*, vol. 43, no. 6, pp. 181–191, Dec. 2001.

[11] N. Blaunstein and J. B. Andersen, *Multipath Phenomena in Cellular Networks*. Norwood, MA: Artech House, 2002.

[12] L. Piazzi and H. L. Bertoni, "Effect of terrain on path loss in urban environments for wireless applications," *IEEE Trans. Antennas Propag.*, vol. 46, no. 8, pp. 1138–1147.

[13] E. Topuz, E. Niver, and L. Felsen, "Electromagnetic fields near a concave perfectly reflecting cylindrical surface," *IEEE Trans. Antennas Propag.*, vol. 30, no. 2, pp. 280–292, March 1982.

[14] T. Ishihara and L. Felsen, "High-frequency propagation at long ranges near a concave boundary," *Radio Sci.*, vol. 23, no. 8, pp. 997–1012, Nov.–Dec. 1988.

[15] A. Beilis and F. D. Tappert, "Coupled mode analysis of multiple rough surface scattering," *J. Acoust. Society Amer.*, vol. 66, 1979.

[16] L. B. Felsen and N. Markuvitz, *Radiation and Scattering of Waves*, 2nd ed. Englewood Cliffs, NJ: Prentice-Hall, 1973.

[17] R. E. Collin, *Field Theory of Guided Waves*. New York: IEEE Press, 1991.

[18] L. M. Brekhovskikh and Y. P. Lysanov, *Fundamentals of Ocean Acoustics*, 2nd ed. Berlin, Germany: Springer-Verlag, 1990.

[19] M. Abramowitz and I. A. Stegun, *Handbook of Mathematical Functions With Formulas, Graphs, and Mathematical Tables*. New York: Dover, 1972.

[20] A. D. Pierce, "Acoustics: An introduction to its physical principles and applications," *Acoust. Soc. Amer.*, 1991.

[21] A. E. Barrios, "A terrain parabolic equation model for propagation in the troposphere," *IEEE Trans. Antennas Propag.*, vol. 42, no. 1, pp. 90–98, Jan. 1994.

[22] A. E. Barrios, K. Anderson, G. Lindem, and G. , "Low altitude propagation effects—A validation study of the advanced propagation model (APM) for mobile radio applications," *IEEE Trans. Antennas Propag.*, vol. 54, no. 10, pp. 2869–2877, Oct. 2006.

[23] D. Dockery and J. R. Kuttler, "An improved impedance-boundary algorithm for Fourier split-step solutions of the parabolic wave equation," *IEEE Trans. Antennas Propag.*, vol. 44, no. 12, pp. 1592–1599, Dec. 1996.

[24] D. J. Donohue and J. R. Kuttler, "Propagation modeling over terrain using the parabolic wave equation," *IEEE Trans. Antennas Propag.*, vol. 48, no. 2, pp. 260–277, Feb. 2000.

Dmitry Chizhik received the Ph.D. degree in electrophysics at the Polytechnic University, Brooklyn, NY. His thesis work has been in ultrasonics and non-destructive evaluation.

He joined the Naval Undersea Warfare Center, New London, CT, where he did research in scattering from ocean floor, geoacoustic modeling of porous media and shallow water acoustic propagation. In 1996, he joined Bell Laboratories, Holmdel, NJ, working on radio propagation modeling and measurements, using deterministic and statistical techniques. He has worked on measurement, modeling and channel estimation of MIMO channels. The results are used both for determination of channel-imposed bounds on channel capacity, system performance, as well as for optimal antenna array design. His recent work has included system and link simulations of satellite and femto cell radio communications that included all aspects of the physical layer. His research interests are in acoustic and electromagnetic wave propagation, signal processing, communications, radar, sonar, medical imaging.

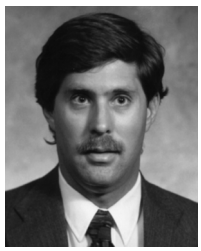

Lawrence Drabeck received the Ph.D. degree in physics from the University of California Los Angeles.

He joined Bell Laboratories, Holmdel, NJ, in 1992 where his initial work was focused on RF properties and potential wireless applications of high-temperature superconductors. He has also worked on next generation radio front ends, interference modeling and smart antennas. He is now part of the Bell Labs E2E Wireless Networking Group where he works on real time network monitoring and optimization.

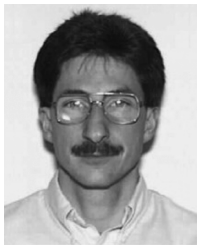

W. Michael MacDonald received the B.S. degree in physics from The University of Notre Dame, New York, in 1979, and the M.S. and Ph.D. degrees in physics from the University of Illinois at Urbana-Champaign, in 1980 and 1984, respectively.

He joined the research staff at AT&T Bell Laboratories, Holmdel, NJ, in 1984 and has been with Bell-Labs since then. He has worked on optical as well as wireless communications topics.